SUPPLEMENTARY MATERIALS

APPENDIX S1. LA-ICP-MS MAJOR AND TRACE ELEMENT ANALYSIS

Instrumentation

In situ major and trace element determination was carried out using a Nu AttoM single-collector ICP-MS (Nu instruments, Wrexham, UK) coupled to a NWR-193 laser-ablation system (ESI, Portland, USA), that utilizes a 193 nm ArF excimer laser, at Department of Geology and Mineralogy, Kyoto University. A full list of instrumental parameters is given in Supplementary Table S1. The laser was operated with an output energy of ~9.0 mJ per pulse, repetition rate of 5 Hz and laser spot size of 35 μm in diameter, providing an estimated power density of the sample of <2.6 Jcm^{-2}. The pulse count was 900 shots. The ablation occurs in He gas within a micro cell, and then the ablated sample aerosol and He gas were mixed with Ar gas downstream of the cell. The He minimizes redeposition of ejecta or condensates, whereas Ar provides efficient sample transport to the ICP-MS (Eggins *et al*., 1998; Gunther and Heinrich, 1999; Jackson *et al*., 2004). The signal-smoothing device was applied to minimize the introduction of large aerosols into the ICP, reducing signal spikes (Tunheng and Hirata, 2004). The Hg-trap device with an activated charcoal filter was applied to the Ar make-up gas before mixing with He carrier gas (Hirata *et al*., 2005).

Data acquisition and reduction

The LA-ICP-MS was optimized using continuous ablation of a NIST SRM 610 to provide maximum sensitivity, especially for rare earth elements (Supplementary Table S2), while maintaining low oxide formation (^{248}ThO/^{232}Th < 1%). Data were acquired on 46 isotopes (Table S2), using the low-resolution linked scan mode and the instruments's time-resolved analysis program. The linked scan mode measures the signal intensity at the peak top over full mass range combining magnet scan with fast scan ion optics. Small number of sweeps (10 sweeps) was selected, resulting in 2.2 seconds per cycle, to use the fast scanning capabilities of the instrument and to gain as much information as possible about the short transient signal during ablation. The time-resolved analysis allows us to easily identify isotopic heterogeneity due to inclusions and a compositional zoning within the ablation volume.

Prior to each individual analysis, regions of interest were pre-ablated using a few pulses of the laser with laser spot size of 50 μm to remove potential surface contamination. Background and ablation data for each analysis were collected over ~60 seconds (Table S1). Backgrounds were measured after pre-ablation prior to each ablation with the laser shutter closed and employing identical settings and gas flows to those used during ablation. Data were acquired in a batch of ~3 hours in duration, consisting of multiple groups of two BCR-2G and eight GA1 analyses bracketed by two NIST SRM 610 analyses. The NIST SRM 610 was used as an external standard. The composition of NIST SRM 610 used for the external calibration is GeoReM preferred values of NIST SRM 610 (Dec/09 (050509)), which are available from the GeoReM database (Jochum and Nohl, 2008) of http://georem.mpch-mainz.gwdg.de. ^{44}Ca was used as an internal standard instead of ^{42}Ca and ^{43}Ca, which have similar sensitivity to that of ^{44}Ca, because the higher intensity for ^{44}Ca results in the higher signal to noise ratio (SNR) for ^{44}Ca (Table S2). Additionally, the intensity ratios of ^{44}Ca/^{42}Ca and ^{44}Ca/^{43}Ca obtained for NIST SRM 610, BCR-2G and GA1 are 3.1–3.3 and 15–16, respectively, comparable to the isotopic abundance ratios of 3.2 and 15, respectively. Thus polyatomic interferences, for example by ^{40}Ca^{4}He and ^{28}Si^{16}O on ^{44}Ca and ^{27}Al^{16}O on ^{43}Ca, may be neglected. The Ca contents for the GA1 were previously determined with EPMA (Fukuyama *et al*., 2007). The averaged value for the Ca contents (36.6 wt.%) was used because the GA1 is homogeneous in Ca within the grain. This double normalization to an internal and external standards allows precise correction for variations in instrument and ablation yield as well as instrumental drift (Longerich *et al*., 1996). BCR-2G was used as a secondary standard for data quality control and the results

Table S1. Instruments settings

Nu AttoM single collector ICP-MS	
RF power	1300 W
Cooling gas flow rate	13 Lmin^{-1}
Auxiliary gas flow rate	0.9 Lmin^{-1}
Detection system	Mixed attenuation-ion counting
IC dead time	18 nsec.
Analytical mode	Linked scan
Number of sweeps	10 sweeps
Time per cycle	2.2 sec.
NWR193 excimer laser system	
ATLEX-SI ArF excimer laser	
Wavelength	193 nm
Pulse energy	~9.0 mJ
Pulse width	4–6 nsec.
Energy density/Fulence	<2.6 Jcm^{-2}
Repeatition rate	5 Hz
Spot diameter	35 μm for analysis
	50 μm for pre-ablation
Helium carrier gas flow rate	0.7 Lmin^{-1}
Argon make-up gas flow rate	0.8 Lmin^{-1}
Effective cell volume	<1 mL
Signal smoothing device	w/
Number of laser shots	900 shots

Table S2. List of chosen isotopes, mean intensities, signal to noise ratios, sensitivities and background equivalent concentrations

Element	Isotope	Gas blank	NIST SRM 610		BCR-2G		GA1		Sensitivity[c] (cps/ppm)	BEC[d] (ppm)
		Mean intensity (cps)	Mean intensity[a] (cps)	SNR[b]	Mean intensity[a] (cps)	SNR[b]	Mean intensity[a] (cps)	SNR[b]		
Li	7	4200	33000	6.9	5200	0.24	4400	0.048	64	65
Na	23	2500000	46000000	17	14000000	4.6	2600000	0.040	440	5700
Mg	25	1980	15600	6.88	708000	357	76200	37.5	293	6.76
Al	27	250000	2270000	8.1	19500000	77	28100000	110	187	1300
P	31	16600	37500	1.26	97200	4.86	18290	0.102	60.9	272
Ca	42[e]	78600	361000	3.59	276000	2.51	1106000	13.1	531	148
Ca	43[e]	10000	66000	6	51400	4	224000	20	510	20
Ca	44[f]	37000	930000	24	680000	17	3260000	87	520	71
Sc	45	5740	166000	27.9	18920	2.30	13950	1.43	363	15.8
Ti	47	2230	17500	6.85	549000	245	121800	53.6	473	4.72
V	51	5060	296000	57.5	307000	59.7	311000	60.5	660	7.67
Cr	52	204000	403000	0.975	211000	0.0343	234000	0.147	586	348
Mn	55	15800	267000	15.9	1011000	63.0	1411000	88.3	518	30.5
Fe	57	25000	30000	0.2	1288000	51	40000	1	500	49
Co	59	11200	237000	20.2	34000	2.0	11600	0.0357	558	20.1
Ni	60	132000	188000	0.424	131000	—	128000	—	466	284
Cu	63	2890	140000	47	9490	2.28	2920	0.0104	460	6.27
Zn	66	640	45000	69	15700	24	671	0.048	350	1.8
Ga	69	2070	207000	99.0	25500	11.3	13840	5.69	778	2.66
Rb	85	5680	250000	43	36700	5.46	5710	0.00528	800	7.14
Sr	88	4500	254000	55	195000	42	5280	0.17	586	7.7
Y	89	4000	180000	40	17900	3	65800	20	390	10
Zr	90	4700	92000	19	44100	8.4	13390	1.8	390	12
Nb	93	5300	217000	40	12090	1.3	5350	0.0094	505	10
Sn	120	585	118000	201	1172	1.00	599	0.0239	910	0.643
Cs	133	3900	290000	73	5170	0.33	3900	0.0	790	4.9
Ba	137	220	30000	100	50700	230	217	—	600	0.36
La	139	56	194000	3500	12700	230	86	0.54	425	0.13
Ce	140	22	250000	11000	33000	1500	650	29	630	0.035
Pr	141	26	250000	9600	4280	160	369	13	580	0.045
Nd	146	7	38000	5000	2910	400	660	90	510	0.01
Sm	147	7	32000	5000	550	80	528	70	470	0.01
Eu	153	20	130000	6000	680	30	1220	60	540	0.04
Gd	157	43	30000	700	520	11	950	21	400	0.10
Tb	159	14	199000	14000	500	40	1380	98	449	0.031
Dy	163	1.4	49000	35000	760	540	2710	1900	460	0.0030
Ho	165	0.7	197000	300000	570	800	2560	4000	439	0.002
Er	166	0.6	65000	100000	550	900	2720	5000	460	0.001
Tm	169	20	198000	10000	270	10	1330	70	471	0.04
Yb	172	2	47000	20000	380	200	2290	1000	490	0.004
Lu	175	16	189000	12000	227	13	1360	84	446	0.036
Hf	178	2	50000	20000	610	300	219	100	400	0.005
Ta	181	9	182000	20000	358	40	9	0	403	0.02
W	182	1	68000	70000	92	90	0.0000002	—	580	0.002
Re	185	116	15000	130	126	0.0862	123	0.0603	850	0.137
Au	197	12	8100	670	15.3	0.28	10.9	—	350	0.034
Pb	208	76	180000	2400	4600	60	70	—	810	0.094
Th	232	0.6	230000	400000	3400	6000	0.2	—	500	0.001
U	238	0.5	380000	800000	1610	3000	28	60	830	0.001

[a]*Mean intensity for samples including both signal and noise.*
[b]*Signal to noise ratio = (mean intensity for sample – mean intensity for gas blank)/mean intensity for gas blank.*
[c]*Sensitivity determined for each isotope in NIST SRM 610.*
[d]*Background equivalent concentration = mean intensity for gas blank/sensitivity.*
[e]*Not used for this study.*
[f]*Used as an internal standard for major and trace element determination.*

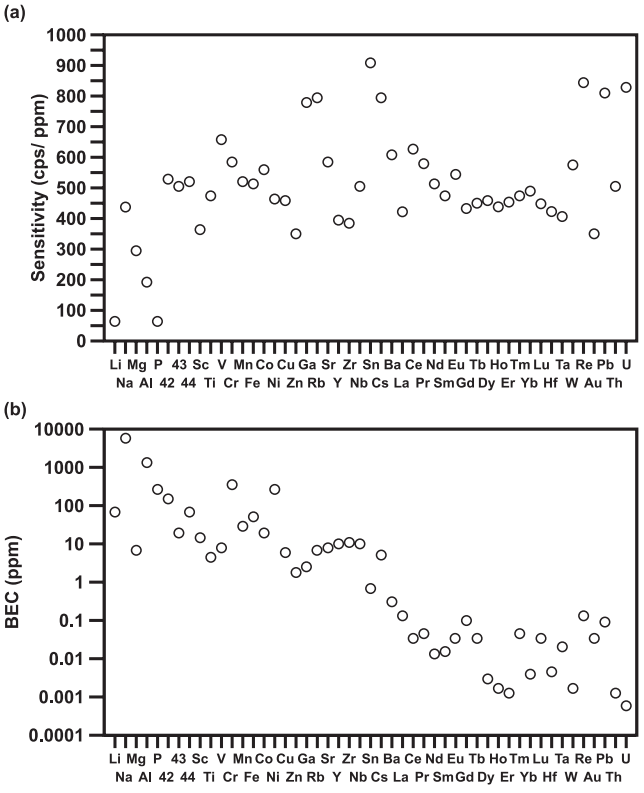

Fig. S1. (a) Sensitivity determined for each isotope in NIST SRM 610 and (b) background equivalent concentration (BEC). Note that 42, 43 and 44 represent ^{42}Ca, ^{43}Ca, ^{44}Ca, respectively, and other isotopes are represented using element name.

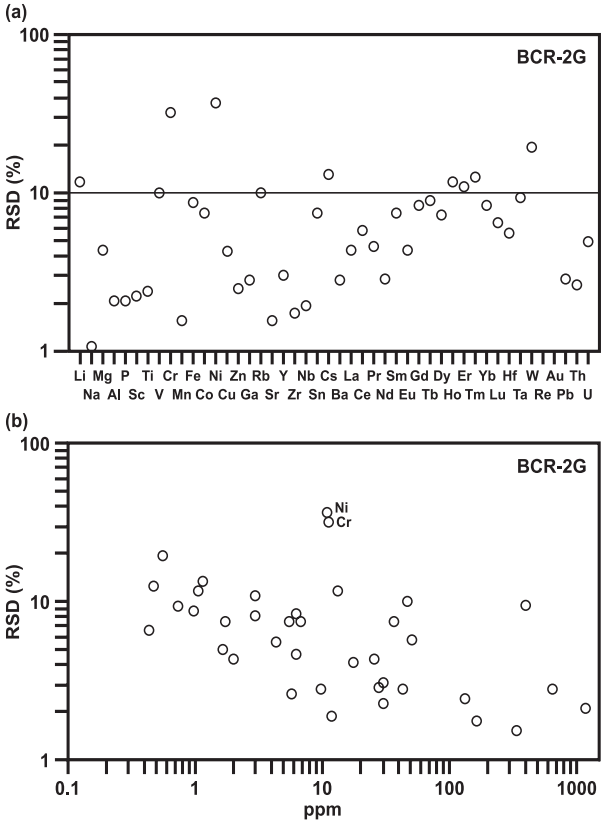

Fig. S2. (a) Relative standard deviation (RSD) for elements determined in BCR-2G and (b) correlation between RSD and element concentration determined in BCR-2G.

of LA-ICP-MS analysis for BCR-2G are discussed later.

All data reduction was conducted off-line using the Iolite data reduction package (Hellstrom *et al*., 2008; Paton *et al*., 2011; see Iolite website: http://iolite.earthsci.unimelb.edu.au/), which runs within the Wavemetrics Igor Pro data analysis software, and following trace element data reduction scheme of Woodhead *et al*. (2007, 2008). Background and external standard (NIST SRM 610) intensities were interpolated between selected time periods using a smoothed cubic spline. For each selected time period for background, external standard and samples (BCR-2G and GA1), the mean and standard error of the measured ratios were calculated rejecting 2 standard deviation outliers.

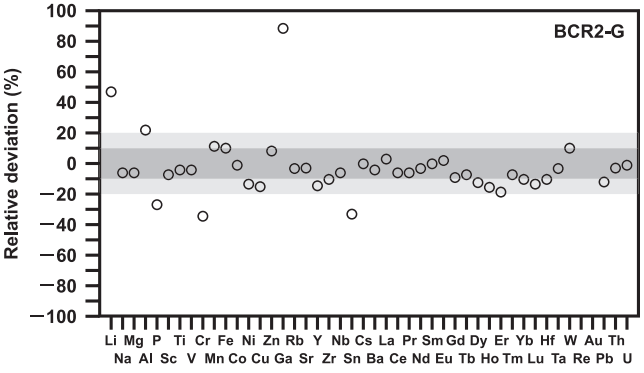

Fig. S3. Relative deviation of average concentrations in BCR-2G determined in this study from the GeoReM preferred values.

Sensitivity and background equivalent concentration

The instrumental settings in this study provide a high sensitivity ranging from 350 to 910 cps/ppm for the analyzed isotopes, except for ^{7}Li (64 cps/ppm), ^{25}Mg (293 cps/ppm), ^{27}Al (187 cps/ppm) and ^{31}P (60.9 cps/ppm), and a background equivalent concentration (BEC) ranging from 0.001 to 5700 ppm, which broadly decreases with increasing atomic number (Table S2; Supplementary Fig. S1). The low sensitivities for the above isotopes may be due to oxide formation for Li, Mg and Al and high ionization energy for P. The high BEC for ^{23}Na (5700 ppm) and ^{27}Al (1300 ppm) suggests the polyatomic interferences with the $^{7}Li^{16}O$ and $^{11}B^{16}O$, respectively, which probably stem from contamination in the instruments.

Table S3. Major and trace element concentrations (ppm) for BCR-2G

Element	This study								GeoReM
	Isotope	Averaged value (ppm)	±1σ	RSD[a] (%)	N[b]	Averaged LOD[c] (ppm)	±1σ	Relative deviation[d] (%)	Prefferred value[e] (ppm)
Li	7	13	2	12	10	9	2	47	9
Na	23	22400	200	1	10	500	200	−7	24000
Mg	24	20200	900	4	10	10	10	−6	21500
Al	27	87000	2000	2	10	30	10	23	70900
P	31	1180	30	3	10	8	3	−26	1600
Sc	45	30.6	0.7	2	10	1.7	0.2	−7	33
Ti	47	13000	300	2	10	9	3	−4	13600
V	51	400	40	10	10	0.6	0.1	−6	425
Cr	52	11	4	32	10	3.2	0.6	−35	17
Mn	55	1640	30	2	10	2.0	0.7	9	1500
Fe	56	106000	9000	8	10	30	20	10	96400
Co	59	37	3	8	10	1.7	0.7	−2	38
Ni	60	11	4	36	5	8	3	−14	13
Cu	63	17.8	0.7	4	10	1.3	0.4	−15	21
Zn	66	136	3	2	10	1.6	0.3	9	125
Ga	69	43	1	3	10	0.5	0.1	89	23
Rb	85	45	5	10	10	0.7	0.2	−3	47
Sr	88	333	5	2	10	1.2	0.2	−3	342
Y	89	29.9	0.9	3	10	2.0	0.5	−15	35
Zr	90	164	3	2	10	3.0	0.5	−11	184
Nb	93	11.7	0.2	2	10	0.7	0.2	−6	13
Sn	118	1.7	0.1	7	10	0.30	0.06	−33	3
Cs	133	1.2	0.2	13	10	0.4	0.1	0	1
Ba	137	650	20	3	10	2	2	−5	683
La	139	25	1	4	10	0.23	0.08	3	25
Ce	140	50	3	6	10	0.2	0.1	−6	53
Pr	141	6.3	0.3	5	10	0.09	0.04	−6	7
Nd	146	27.9	0.8	3	10	0.3	0.2	−4	29
Sm	147	6.6	0.5	7	10	0.3	0.1	0	7
Eu	153	2.00	0.09	4	10	0.09	0.02	1	2
Gd	157	6.1	0.5	8	10	0.8	0.3	−9	7
Tb	159	0.95	0.08	9	10	0.07	0.04	−7	1
Dy	163	5.6	0.4	7	10	0.06	0.08	−13	6
Ho	165	1.1	0.1	12	10	0.04	0.05	−16	1
Er	166	3.0	0.3	11	10	0.1	0.1	−19	4
Tm	169	0.47	0.06	13	10	0.09	0.03	−7	1
Yb	172	3.0	0.2	8	10	0.1	0.1	−11	3
Lu	175	0.43	0.03	7	10	0.08	0.03	−14	1
Hf	178	4.3	0.2	5	10	0.1	0.1	−11	5
Ta	181	0.75	0.07	9	10	0.09	0.07	−4	1
W	182	0.6	0.1	19	9	0.04	0.08	10	1
Re	185	<LOD	—	—	—	0.14	0.03	—	0
Au	197	0.037	0	0	1	0.04	0.02	—	—
Pb	208	9.7	0.3	3	10	0.11	0.03	−12	11
Th	232	5.7	0.1	3	10	0.01	0.01	−3	6
U	238	1.67	0.08	5	10	0.00	0.01	−1	2

[a] *1 sigma relative standard deviation.*
[b] *Number of analysis used for estimate of averaged values.*
[c] *Limit of detection averaged for 10 repeated analyses.*
[d] *Relative deviation of averaged concentrations determined in BCR-2G from the GeoReM preferred values.*
[e] *GeoReM preferred values of BCR-2G (1/2009; Jochum (Max-Planck-Institute fuer Chemie)) are from the GeoReM database (Jochum and Nohl, 2008) of http://georem.mpch-mainz.gwdg.de*

Table S4. Major and trace element concentrations (ppm) for GA1

Element	This study (NIST SRM 610 as external standard)							Fukuyama *et al.* (2007)[d]			
	Isotope	Averaged value (ppm)	±1σ	RSD[a] (%)	N[b]	Averaged LOD[c] (ppm)	±1σ	Averaged value (ppm)	±1σ	RSD[a] (%)	N[b]
Li	7	<LOD	—	—	—	8	2	5	3	53	3
Na	23	<LOD	—	—	—	300	300	—	—	—	—
Mg	24	2200	100	5	34	8	2	2000	200	10	3
Al	27	130000	3000	2	34	30	30	116400	300	0	3
P	31	25	4	15	34	7	2	—	—	—	—
Ca[e]	44	—	—	—	—			262000	1000	0	3
Sc	45	19.9	0.6	3	34	1.8	0.6	35	3	9	3
Ti	47	2990	70	2	34	7	2	<100	—	—	3
V	51	430	60	14	34	0.7	0.2	370	10	3	3
Cr	52	60	10	17	34	3.4	0.8	<100	—	—	3
Mn	55	2380	60	3	34	2	2	2000	200	10	3
Fe	56	1400	100	7	34	18	4	800	200	25	3
Co	59	<LOD	—	—	—	1.7	0.6	20	5	24	3
Ni	60	<LOD	—	—	—	7	2	—	—	—	—
Cu	63	<LOD	—	—	—	1.0	0.3	9	5	58	3
Zn	66	<LOD	—	—	—	1.6	0.4	8	8	98	3
Ga	69	22.9	0.8	3	34	0.5	0.1	18	1	6	3
Rb	85	<LOD	—	—	—	0.7	0.1	0.9	0.3	29	2
Sr	88	1.3	0.3	25	18	1.2	0.4	1.7	0.9	52	3
Y	89	135	4	3	34	2.0	0.4	148	3	2	3
Zr	90	38	1	4	34	2.7	0.8	41	4	9	3
Nb	93	<LOD	—	—	—	0.7	0.2	0.5	0.4	76	3
Sn	118	<LOD	—	—	—	0.3	0.1	4	2	40	3
Cs	133	<LOD	—	—	—	0.4	0.1	0.7	0.4	64	3
Ba	137	<LOD	—	—	—	1.6	0.4	2.93	0.00	0	1
La	139	0.21	0.03	17	13	0.19	0.07	0.26	0.07	29	3
Ce	140	1.0	0.1	14	34	0.14	0.09	1.0	0.1	13	3
Pr	141	0.56	0.05	8	34	0.07	0.02	0.5	0.1	22	3
Nd	146	6.7	0.4	7	34	0.2	0.1	6.1	0.6	9	3
Sm	147	6.7	0.3	5	34	0.3	0.2	7	2	23	3
Eu	153	3.8	0.2	4	34	0.09	0.03	3.2	0.7	22	3
Gd	157	11.8	0.6	5	34	0.8	0.2	12.0	0.7	6	3
Tb	159	2.7	0.2	6	34	0.06	0.03	2.9	0.3	10	3
Dy	163	20.8	0.8	4	34	0.09	0.09	21.3	0.7	3	3
Ho	165	5.1	0.3	6	34	0.03	0.05	5.5	0.3	5	3
Er	166	15.5	0.7	5	34	0.1	0.1	17	1	9	3
Tm	169	2.5	0.1	5	34	0.08	0.04	2.6	0.1	5	3
Yb	172	18.9	0.9	5	34	0.2	0.1	21.5	0.8	4	3
Lu	175	2.8	0.1	3	34	0.08	0.03	2.7	0.2	9	3
Hf	178	1.7	0.2	10	34	0.1	0.1	1.6	0.4	27	3
Ta	181	<LOD	—	—	—	0.09	0.05	0.5	0.1	30	3
W	182	<LOD	—	—	—	0.1	0.1	0.5	0.4	72	2
Re	185	<LOD	—	—	—	0.16	0.04	—	—	—	—
Au	197	<LOD	—	—	—	0.04	0.02	—	—	—	—
Pb	208	<LOD	—	—	—	0.09	0.03	0.43	0.05	13	3
Th	232	0.002	0.002	66	6	0.002	0.004	0.3	0.1	37	2
U	238	0.030	0.004	15	34	0.002	0.004	0.09	0.00	0	1

[a] *1 sigma relative standard deviation.*
[b] *Number of analysis used for estimate of averaged values.*
[c] *Limit of detection averaged for 34 repeated analyses.*
[d] *Concentrations in the GA1 were determined with LA-ICP-MS, except for those of Mg, Al, Ca, Ti, Cr, Mn and Fe determined with EPMA.*
[e] *^{44}Ca was used as internal standard.*

However, the $^{7}Li^{16}O$ from NIST SRM 610 and BCR-2G does not significantly increase the intensity of ^{23}Na because of high Na concentrations in the samples. The aluminum oxide formation (e.g., $^{27}Al^{16}O$) does not cause the polyatomic interferences on ^{43}Ca, as discussed above.

BCR-2G

Analytical results of BCR-2G used are listed with precision as 1 s relative standard deviation (RSD) in Supplementary Table S3. Data on the limits of detection (LOD) are also given in Table S3. For comparison, GeoReM preferred values of BCR-2G (1/2009; Jochum (Max-Planck-Institute fuer Chemie)) are also listed in Table S3. The GeoReM preferred values are available from the GeoReM database (Jochum and Nohl, 2008).

Two elements (Re and Au) out of 46 elements analyzed for the BCR-2G have concentrations below the LOD (Table S3). The RSD for other 44 major and trace elements is generally better than 10% for most elements, except for Li (12%), Cr (32%), Ni (36%), Cs (13%), Ho (12%), Er (11%), Tm (13%) and W (19%) (Table S3; Supplementary Fig. S2a). The high RSD for the above elements is due to very low concentrations in the case of Cs (1.2 ppm), Ho (1.1 ppm), Er (3.0 ppm), Tm (0.5 ppm) and W (0.6 ppm). Although the Li (13 ppm), Cr (11 ppm) and Ni (8 ppm) have higher concentrations, their SNR are low (Li = 0.24, Cr = 0.0343, Ni < 0; Table S2). This is one of the reasons for the high RSD.

Elements in BCR-2G with concentrations less than 1500 ppm show negative correlation between concentration and RSD on a logarithmic scale with a logarithmic correlation coefficient of –0.74 (R^2 = 0.1628; Fig. S2b), which is similar to that estimated from the results of LA-ICP-MS analysis for BCR-2G with the laser spot of 60 μm by Gao *et al*. (2002; a logarithmic correlation coefficient of –0.76). This trend indicates that the difference in the scatter of apparent element concentrations is not by chemical heterogeneity but counting statistics, suggesting that BCR-2G is overall homogeneous on a scale resolution of 35 μm, as shown by previous studies (Gao *et al*., 2002; Norman *et al*., 1998; Rocholl, 1998). However, Cr and Ni with high RSD do not follow the trend whereas concentrations of these elements determined by Gao *et al*. (2002) show lower RSD and follow the trend in Gao *et al*. (2002). These lines of evidence may suggest that BCR-2G is unlikely homogeneous in concentrations of Cr and Ni on this scale resolution. Alternatively, their lower SNR could result in the outliers.

Most of element concentrations in BCR-2G determined in this study agree with the GeoReM preferred values of BCR-2G within ±20% relative (Table S3; Supplementary Fig. S3). Exceptions are Li (+47%), Al (+22%), P (–27%), Cr (–35%), Ga (+89%) and Sn (–33%). However, Cr is consistent with the reference value within error (2sd). It should be noted that Sn (1.7 ppm) is relatively low concentrations in BCR-2G.

The agreement between the reference and obtained values for Na, Mg, Ti and Fe in BCR-2G as well as trace elements demonstrates the quantification capability of the LA-ICP-MS system up to concentrations of at least several weight percent due to its extended detector dynamic range of 10^9. The wide dynamic range extends the possibility of major element measurements with LA-ICP-MS and the use of multiple internal standards.

REFERENCES

Eggins, S. M., Kinsley, L. P. J. and Shelley, J. M. G. (1998) Deposition and element fractionation processes during atmospheric pressure laser sampling for analysis by ICP-MS. *Appl. Surf. Sci*. **129**, 278–286.

Fukuyama, M., Ogasawara, M., Sato, H. and Ishiyama, D. (2007) Trace element analysis of gem garnet by LA-ICP-MS: preliminary evaluation as micro-beam standard. *Bull. Geol. Surv. Jpn*. **58**, 93–103.

Gao, S., Liu, X., Yuan, H., Hattendorf, B., Gunther, D., Chen, L. and Hu, S. (2002) Determination of forty two major and trace elements in USGS and NIST SRM glasses by laser ablation-inductively coupled plasma-mass spectrometry. *Geostand. Newsl. J. Geostand. Geoanal*. **26**, 181–196.

Gunther, D. and Heinrich, C. A. (1999) Enhanced sensitivity in laser ablation-ICP mass spectorometry using helium-argon mixtures as aerosol carrier. *J. Anal. At. Spectrom*. **14**, 1363–1368.

Hellstrom, J., Paton, C., Woodhead, J. D. and Hergt, J. M. (2008) Iolite: software for spatially resolved LA-(quad and MC)-ICPMS analysis. *Laser Ablation ICP-MS in the Earth Sciences: Current Practices and Outstanding Issues* (Sylvester, P., ed.), *Mineralogical Association of Canada Short Course Series* **40**, 343–348.

Hirata, T., Iizuka, T. and Orihashi, Y. (2005) Reduction of mercury background on ICP-mass spectrometry for *in situ* U-Pb age determinations of zircon samples. *J. Anal. At. Spectrom*. **20**, 696–701.

Jackson, S. E., Pearson, N. J., Griffin, W. L. and Belousova, E. A. (2004) The application of laser ablation-inductively coupled plasma-mass spectrometry to in situ U-Pb zircon geochronology. *Chem. Geol*. **211**, 47–69.

Jochum, K. P. and Nohl, U. (2008) Reference materials in geochemistry and environmental research and the GeoReM database. *Chem. Geol*. **253**, 50–53.

Longerich, H. P., Jackson, S. E. and Gunther, D. (1996) Laser ablation inductively coupled plasma mass spectrometric transient signal data acquisition and analyte concentration calculation. *J. Anal. At. Spectrom*. **11**, 899–904.

Norman, M. D., Griffin, W. L., Pearson, N. J., Garcia, M. O. and O'Reilly, S. Y. (1998) Quantitative analysis of trace element abundances in glasses and minerals: a comparison of laser ablation inductively coupled plasma mass spectrometry, solution inductively coupled plasma mass spectrometry, proton microprobe and electron microprobe data. *J. Anal. At. Spectrom*. **13**, 477–482.

Paton, C., Hellstrom, J., Paul, B., Woodhead, J. and Hergt, J. (2011) Iolite: Freeware for the visualisation and processing of mass spectrometric data. *J. Anal. At. Spectrom*. **26**, 2508–2518.

Rocholl, A. (1998) Major and trace element composition and homogeneity of microbeam reference material: basalt glass USGS BCR-2G. *Geostand. Newsl. J. Geostand. Geoanal*. **22**, 33–45.

Tunheng, A. and Hirata, T. (2004) Development of signal smoothing device for precise elemental analysis using laser ablation-ICP-mass spectorometry. *J. Anal. At. Spectrom*. **19**, 932–934.

Woodhead, J. D., Hellstrom, J., Hergt, J., Greig, A. and Maas, R. (2007) Isotopic and elemental imaging of geological materials by laser ablation inductively coupled plasma mass spectrometry. *Geostand. Geoanal. Res*. **31**, 331–343.

Woodhead, J. D., Hellstrom, J., Paton, C., Hergt, J. M., Greig, A. and Maas, R. (2008) A guid to depth profiling and imaging applications of LA-ICP-MS. *Laser Ablation ICP-MS in the Earth Sciences: Current Practices and Outstanding Issues* (Sylvester, P., ed.), *Mineralogical Association of Canada Short Course Series* **40**, 135–145.